Since January 2020 Elsevier has created a COVID-19 resource centre with free information in English and Mandarin on the novel coronavirus COVID-19. The COVID-19 resource centre is hosted on Elsevier Connect, the company's public news and information website.

Biomedical Signal Processing and Control 78 (2022) 103920

Contents lists available at ScienceDirect

Biomedical Signal Processing and Control

journal homepage: www.elsevier.com/locate/bspc

A comparison of the power of breathing sounds signals acquired with a smart stethoscope from a cohort of COVID-19 patients at peak disease, and pre-discharge from the hospital

Nour Kasim [a], Noa Bachner-Hinenzon [b], Shay Brikman [a,c], Ori Cheshin [a], Doron Adler [b], Guy Dori [a,c,*]

[a] Department of Internal Medicine E and Corona, HaEmek Medical Center, Afula, Israel
[b] Sanolla Ltd. Nesher, Israel
[c] Faculty of Medicine, Technion –Israel Institute of Technology, Haifa, Israel

A B S T R A C T

Objectives: To characterize the frequencies of breathing sounds signals (BS) in COVID-19 patients at peak disease and pre-discharge from hospitalization using a Smart stethoscope.
Methods: Prospective cohort study conducted during the first COVID-19 wave (April-August 2020) in Israel. COVID-19 patients (n = 19) were validated by SARS-Cov-2 PCR test. The healthy control group was composed of 153 volunteers who stated that they were healthy. Power of BS was calculated in the frequency ranges of 0–20, 0–200, and 0–2000 Hz.
Results: The power calculated over frequency ranges 0–20, 20–200, and 200–2000 Hz contributed approximately 45%, 45%, and 10% to the total power calculated over the range 0–2000 Hz, respectively. Total power calculated from the right side of the back showed an increase of 45–80% during peak disease compared with the healthy controls ($p < 0.05$). The power calculated over the back, in the infrasound range, 0–20 Hz, and not in the 20–2000 Hz range, was greater for the healthy controls than for patients. Using all 3 ranges of frequencies for distinguishing peak disease from healthy controls resulted in sensitivity and specificity of 84% and 91%, respectively. Omitting the 0–20 Hz range resulted in sensitivity and specificity of 74% and 67%, respectively.
Discussion: The BS power acquired from COVID-19 patients at peak disease was significantly greater than that at pre-discharge from the hospital. The infrasound range had a significant contribution to the total power. Although the source of the infrasound is not presently clear, it may serve as an automated diagnostic tool when more clinical experience is gained with this method.

1. Introduction

1.1. Background

The SARS-Cov-2 pandemic, more than 2 years after its onset, is still causing local outbreaks, and the respiratory system is the principle system afflicted by the virus. SARS-Cov-2 causes cough and dyspnea, which may deteriorate to acute respiratory failure requiring mechanical ventilation [1–3].

Assessing a patient's clinical status involves lung auscultation. However, in the setting of COVID-19 quarantine wards at the hospital, auscultating breathing sounds (BS) is limited by: (1) the personal protective equipment physicians use, which covers their ears [4], (2) the occasional shortage of physicians who are well-trained in lung auscultation, (3) the diverse characteristics of BS in cases of COVID-19 [4], (4) the "silent" nature of COVID-19 pneumonia [5], and (5) the BS sought may contain low frequencies (i.e. infrasound) which are below the frequency range the human ear can detect [6].

Imaging modalities (e.g. chest CT) are objective and considered the gold standard for detecting COVID-19 related pneumonia; however, radiation exposure, availability and cost precludes its utilization as a screening and follow-up tool for every COVID-19 patient.

In effort to overcome human subjective audio interpretation of BS (normal and adventitious) and standardize BS analysis, much research and progress took place using a variety of sensors and methods of analyses. Pramono et al 2017 and Reichert et al 2008 summarized the state of the art on this topic [7,8]. In COVID-19 pneumonia BS may be auscultated as normal or if adventitious sounds are detected they are usually of the coarse crackle or rhonchi type, both characterized by frequencies of the lower range (<300 Hz) [7,8]. Lapteva et al. conducted a large study using the Lungpass, an automated lung sound analysis platform including a wireless digital stethoscope paired with a mobile

* Corresponding author at: Department of Internal Medicine E and Corona, HaEmek Medical Center, Afula, Israel.
E-mail address: guydo@clalit.org.il (G. Dori).

https://doi.org/10.1016/j.bspc.2022.103920
Received 16 November 2021; Received in revised form 14 June 2022; Accepted 18 June 2022
Available online 27 June 2022

phone application, to detect COVID-19 involvement of the lower respiratory tract, as the latter predicts severe clinical course and outcome. Crackles were the most common adventitious sounds detected by Lungpass. The system performed better than expert pulmonary physicians, identifying crackles over at least one auscultation site in 93.6% of the cases, whereas the physicians identified 74.5%. Lapteva et al. concluded that the sensitivity and specificity of the Lungpass system for detecting abnormal lung sounds in at least two auscultation sites as an indicator of lower respiratory tract COVID-19 disease were 94.0% and 96.9%, respectively [9]. Glangetas at al. reported a study protocol, where deep learning methods (DeepBreath) will be applied to digitized lung sounds in order to diagnose and risk stratify COVID-19 patients [10].

The Smart stethoscope used in this study (VoqX^{TM}, Sanolla Ltd.) to record BS acquired acoustic signals in the range of 6–2000 Hz, thus enabling analysis of the infrasound range (<20 Hz, not audible by human ears). This wide range of frequencies enabled distinguishing between the infrasound range (<20 Hz) and higher frequencies. In particular, we focused on the infrasound range, investigating whether COVID-19 patients expressed greater power in this frequency range. The acquired signals were recorded from patients hospitalized in COVID-19 isolation department and transmitted wirelessly to a digital storage (cloud) for later spectral analysis.

This study was conducted early in the pandemic in order to assess the applicability of using a digital stethoscope and to characterize the frequencies of BS in COVID-19 patients at peak disease and pre-discharge from hospitalization. The frequencies of patients' BS were compared to those of healthy controls and were used to distinguish patients from controls using classification method. The results of this study may help exploring the route toward machine detection of COVID-19 pneumonia.

2. Methods

2.1. COVID-19 patients and healthy controls

A cohort of 19 PCR tested and verified positive COVID-19 patients, were recruited in our Corona department (Corona A, HaEmek medical center, Afula, Israel) from 13.4.2020 to 5.8.2020. Informed consent was provided by each patient (Institutional review board protocol EMC-0160–19). Critically ill patients who could not sign the informed consent were not recruited.

The healthy control (HC) group was composed of healthy volunteers escorting patients to emergency departments in 4 medical centers in Israel. These individuals submitted informed consent prior to participating in the study. In each of the centers, institutional review boards authorized the study (Rambam medical center, Haifa, RMB-0007–17, RMB-0631–18; Assaf harofe medical center, Be'er-Yaacov, ASF-0136–20; Carmel medical center, Haifa, EMC-0075–16; HaEmek medical center, Afula, EMC-0160–19). Recordings of BS from HC were performed prior to the COVID-19 pandemic.

2.2. Study protocol

BS were recorded from the COVID-19 cohort at peak disease (PD), which was defined as the first BS recording session during hospitalization or a latter recording if the patient was evaluated to be in a worse clinical condition. BS were also recorded at pre-discharge from hospital (D) when patients were evaluated to be independent and in good clinical condition.

2.3. Breathing sounds acquisition

BS were recorded using a Smart stethoscope, VoqX^{TM} (Sanolla Inc., Nesher, Israel), from 14 standard anatomical locations over the thorax as depicted by Fig. 1.

2.4. Breathing sounds - signal analysis

Sampling frequency was 16000 Hz. After digitizing BS signals, they were stored in a cloud for later analysis. BS signals underwent the following preprocessing: 1. The first and last second of each BS record (BSR) were trimmed to eliminate the noise generated by either placing or removing the stethoscope from the chest. 2. Background noise was eliminated by using a second microphone integrated in the VoqX^{TM} for recording the ambient noise, thus enabling dynamic noise reduction. 3. Low-pass filter and decimation to sample frequency of 4000 Hz. Each BSR underwent discrete Fourier transform [6]. If the BSR length contained S samples, it was padded with zeros to S1, where S1 was the nearest power of 2 greater than S.

The calculated power (in units of decibel full scale, dBfs) was normalized by the original length of the BSR. The normalized power is abbreviated here as Pn0-2000. Pn0-2000 however, does not indicate the contribution of a range of frequencies to the power of the full spectrum 0–2000 Hz. Therefore, the power was calculated in 3 distinct frequency intervals: 0–20, 0–200, 0–2000 Hz. The following ratios of the powers (RP) were defined: RP0-20 = Pn0-20/Pn0-2000 and RP0-200 = Pn0-200/Pn0-2000. The latter provided the relative contribution of the range 0–20 Hz and 0–200 Hz to Pn0-2000, respectively. Had the BSR been derived from a "white noise" generator, the contribution of each frequency range to the total power, Pn0-2000, would be linearly proportional to the width of the frequency range relative to the whole range 0–2000 Hz. For example, the contribution of the range 0–20 Hz, and 0–200 Hz, would be expected to contribute 1% and 10% to Pn0-2000, respectively.

2.5. Classification

The classification was performed twice by using machine learning support vector machine (SVM) with a Gaussian kernel. Three features were used: RP0-20, RP0-200 and Pn0-2000, followed by using only 2 features, omitting RP0-20. Classification was performed for: six

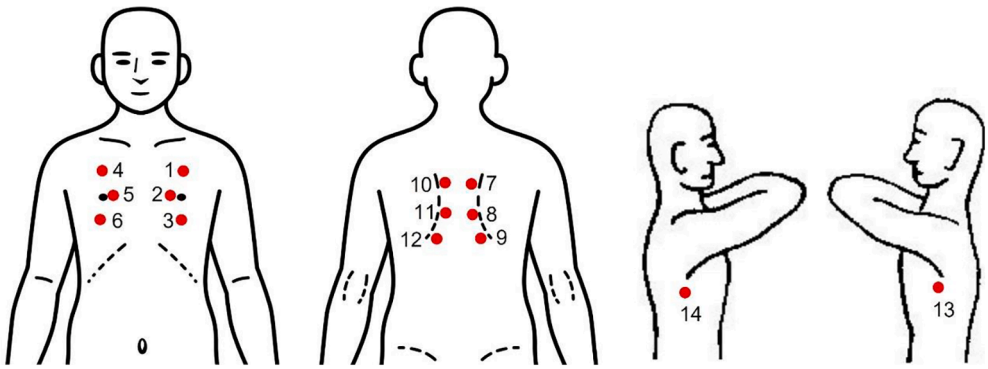

Fig. 1. Standard anatomical thorax locations for breathing sounds recording BS were recorded for at least 4 s at each anatomical location.

anatomical locations on the front chest, six anatomical locations on the back, and 12 locations including the back and front chest points. The performance was evaluated by calculating the sensitivity, specificity and the area under curve (AUC). The comparison between the AUCs was performed using DeLong method [11]. Due to the small amount of data, the classification was performed as a 5-fold cross-validation to show the potential performance of such a classifier.

2.6. Statistical analysis

Variables randomly distributed in a symmetric manner were characterized by means and standard deviations. Student's *t*-test was applied to assess whether means of samples were derived from different samples. $P < 0.05$ defined the level of significance. As some of the variables deviated from symmetric distribution, a non-parametric test (Mann-Whitney) was applied to assess the difference between the groups; however, results were similar to the results of the *t*-test.

3. Results

Nineteen COVID-19 patients, 47.4% females, age 54 ± 12.5 years, were recruited. 68.4% of the patients had co-morbidities such as diabetes mellitus, hypertension, and hyperlipidemia. Table 1 summarizes the clinical and demographic characteristics of the study groups. The HC group was composed of 153 individuals of which 2/3 were males. The study group was older than the control group ($p < 0.003$).

Clinically, patient group was heterogeneous with only a third of the patients having a severe disease.

3.1. The power of BSR in the full range 0–2000 Hz

The Pn0-2000 was calculated for the 3 groups: HC, PD, and D. BS were acquired at 4 anatomical points only (see Fig. 1, points 8,9,11,12) for a subgroup within the HC group (n = 46). We report the power of all 153 HC, as excluding the above 46 subjects from the power calculation did not change the result.

Table 1
Demographic and clinical characteristics of the study groups.

	COVID-19 patients (n = 19)	Healthy controls (n = 153)
Age (years ± s.d.)	54.9 ± 12.5	45 ± 14p = 0.003
Female (%)	9 (47.4)	55 (35.9) p = 0.33
Diabetes mellitus (%)	36.84	
Hypertension (%)	57.89	
COPD (%)	10.5	
Asthma (%)	5.25	
Smokers (%)	10.5	
Severity of COVID-19 disease		
Mild (%)	68.42	
Moderate-severe (%)	31.58	
Time interval between day 1 of hospitalization and day of acquiring breathing sounds at peak disease (days ± s.d.)	2.2 ± 2.42	
Time interval between day of acquiring breathing sounds at peak disease and pre-discharge (days ± s.d.)	8.58 ± 8.67	
Pulmonary infiltrates on chest X-ray (unilateral) (%)	21.05	
Pulmonary infiltrates on chest X-ray (bilateral) (%)	5.26	
Pulmonary ultrasound (presence of B-lines) (%)	31.58	
Pulmonary findings on chest CT (%)	100%	

CT – chest computerized tomography; s.d. – standard deviation.

Fig. 2 shows the power in the whole frequency range 0–2000 Hz, Pn0-2000, for all 3 groups, as a function of the anatomical locations of BS recording.

Fig. 2 shows that Pn0-2000 is greater for BSR acquired at the upper (1, 4) versus lower (3, 6) locations on the front thorax. The values of Pn0-2000 acquired on the front thorax, for the 3 groups, did not differ in a statistically significant manner.

On the back (right side, locations 7,8,9, and left side location 10), Pn0-2000 increased significantly from HC (level of dBfs 80000–100000) to PD (level > 130000). When patient recovered Pn0-2000 decreased towards HC levels. However, Pn0-2000 calculated for D was usually greater than Pn0-2000 of HC. Significant statistical difference ($p < 0.05$) was observed between PD and HC in anatomical locations: 7,8,9,10. Between PD and D a significant statistical difference was noted at location 9. Pn0-2000 calculated for anatomical locations 13, and 14 (mid axillary lines left and right, respectively) resulted in non-significant differences.

As stated above, Pn0-2000 represents the whole power of the BSR, lacking insight to the contributions of frequency ranges to the Pn0-2000. Therefore, RP0-20 and RP0-200 were calculated.

3.2. The ratio of the power of BSR in the infrasound range to the full range 0–2000 Hz (RP0-20)

Fig. 3 shows RP0-20 as a function of the anatomic locations of BS acquisition. It is shown that the contribution to Pn0-2000 of this narrow range, 0–20 Hz (also termed: infrasound) is between 40 and 50%. The latter is greater for HC compared with COVID-19 patients, when BS were recorded on the back. In addition to that, the front thorax anatomical locations did not provide significant information, as the difference in RP0-20 between the 3 groups was not statistically significant. Only at locations 10 and 11 (back, left side), RP0-20 calculated for HC significantly differed from that of patients during PD and D ($p < 0.022$). At location 8 (back, right side) the difference between RP0-20 of HC and D was also statistically significant ($p = 0.036$).

3.3. The ratio of the power of BSR in the 0–200 Hz range to the full range 0–2000 Hz (RP0-200)

Fig. 4 shows RP0-200 as a function of the anatomic locations of BS acquisition. For the 3 study groups, the contribution of the frequency range 0–200 Hz to Pn0-2000 was 85–93%. Thus, the power in the frequency range 20–200 Hz contributed approximately 45% of Pn0-2000. The remaining frequency range 200–2000 Hz contributed 7 to 15% to Pn0-2000. Thus, the contributions of the frequency ranges 0–20 Hz and 0–200 Hz were not proportional to their relative proportion over the whole frequency range 0–2000 Hz. The importance of RP0-200 is in understanding the contribution of this frequency range to Pn0-2000. The values of RP0-200 at the specific anatomical locations did not provide significant information.

3.4. Classification results

Table 2 summarizes the performance of the classifiers. It can be observed that when omitting the RP0-20 feature, the performance is significantly lower on the back and both front and back. The best performance for PD and D detection appears when using anatomical locations on the back.

Fig. 5 shows the receiver operating curves (ROC) for the 5-fold cross-validations of the different classifiers. These curves outline the contribution of the RP0-20 feature in distinguishing between any two states. Generally, the infrasound contribution was greater when BSR were obtained from the back of the patients.

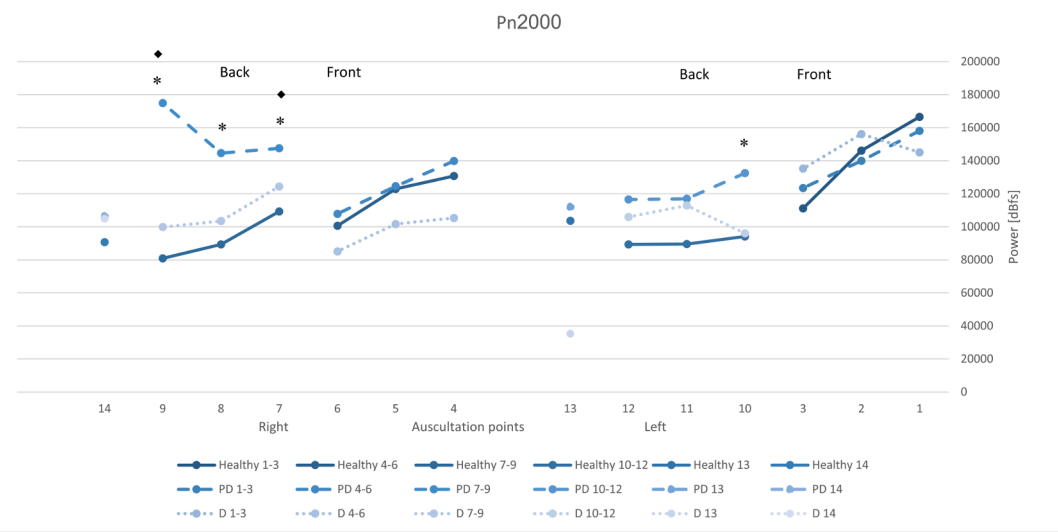

Fig. 2. The power in the whole frequency range 0–2000 Hz for the 3 study groups as a function of the anatomical locations of breathing sounds recording * – $p < 0.05$ power values at peak disease versus healthy controls; ◆– $p < 0.05$ power values at peak disease versus pre-discharge; D – patients pre-discharge from hospital; dBfs – dB full scale; PD – peak disease; Pn0-2000 – the power in the frequency range 0–2000 Hz. The anatomical locations of BSR are given on the abscissa, where locations: 1,2,3,10,11,12,13 are on the left side of the thorax. The mean power is given on the ordinate.

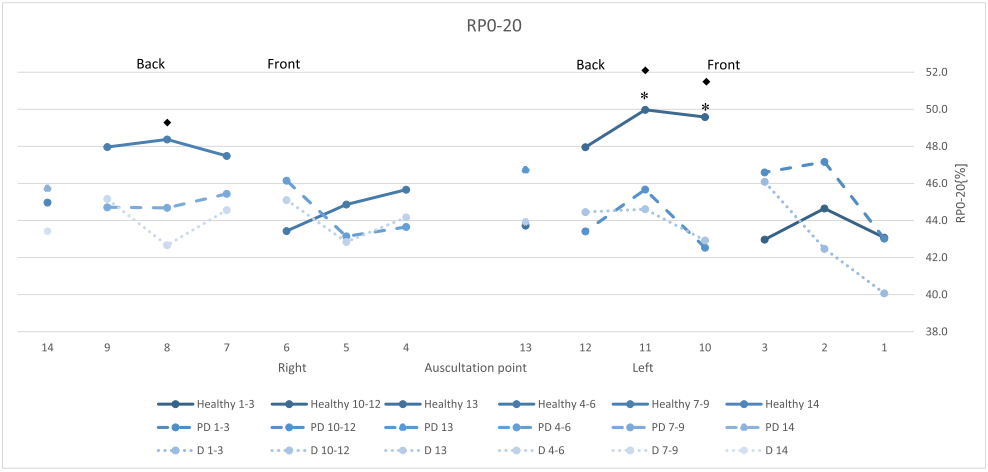

Fig. 3. RP0-20 for the 3 study groups as a function of the anatomical locations of breathing sounds recording, * – $p < 0.05$ RP0-20 healthy controls values versus peak disease; ◆– $p < 0.05$ RP0-20 healthy controls values versus pre-discharge; D – pre-discharge; PD – peak disease; RP0-20 – ratio Pn0-20/Pn0-2000;

4. Discussion

4.1. Main findings

In this study BS were recorded from COVID-19 patients at peak disease (PD) and pre-discharge from hospital (D). Acquiring BS from COVID-19 patients in a quarantine ward was easy to implement as previously reported [12,13] and BSR can be auscultated in real-time with the device and various analyses can be performed off-line. The VoqX^{TM} device helps overcoming the standard auscultation limitations imposed by quarantine conditions. As frequency range of the device is not limited, the VoqX^{TM} provides means to evaluate the infrasound component of the power. Also, the digital stethoscope circumvents the auscultator experience requirement as BSR can be analyzed objectively by a variety of measures [8].

Power analysis showed that the infrasound range, 0–20 Hz, contributed 45–50% of the total power (Pn0-2000). Previous studies, although technically different from ours, demonstrated similar results. Gavriely et al. were the first to report spectral analysis of chest wall breath sounds from healthy subjects [14]. Gross et al. conducted power spectrum analysis of BSR for healthy individuals and showed that most of the power was contributed by frequency range 0–200 Hz [6]. Tsai et al. reported that in healthy subjects the total power was greater on the left side of the back compared with the right side [15]. Our analysis showed similar power of both sides. In addition, power analysis of BSR acquired over the front thorax provides statistically non-significant information. It is possible that body organs such as heart and liver muffle BS.

The power in the frequency range 0–2000 Hz, at locations 7,8,9 (on the right side of the back) during PD increased by 45–80% compared to the power calculated for HC. Pre-discharge from the hospital the power decreased to values similar, but somewhat greater than those of HC. The difference in the power calculated for HC and D was not statistically significant. It is suggested that when BS are recorded from the right side of the back and power is calculated, an increase in power greater than 45% may suggest the presence of COVID-19 pneumonia.

Using the SVM to correctly classify the data into HC, PD and D groups, it was evident that the infrasound range had contributed

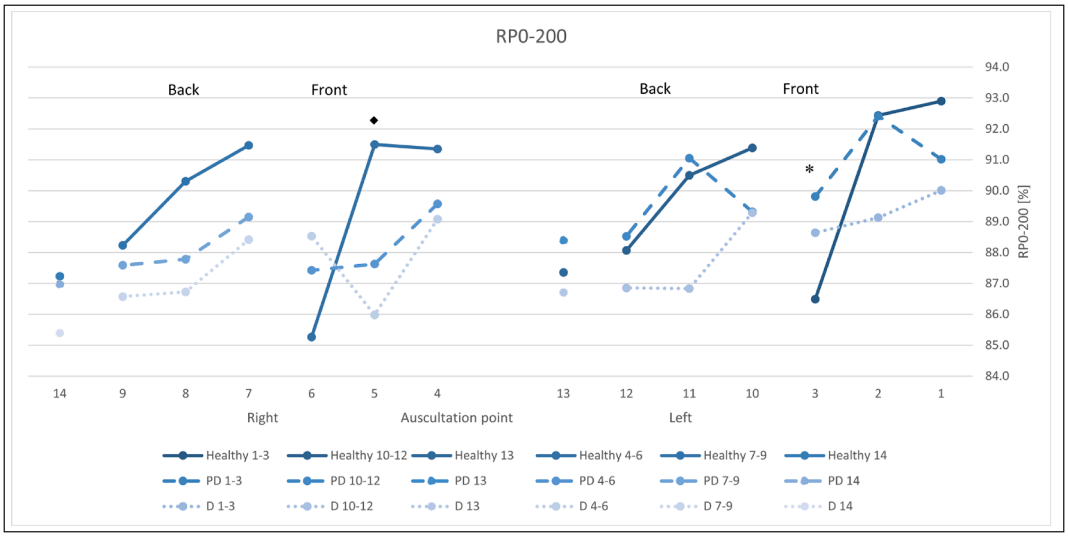

Fig. 4. RP0-200 for the 3 study groups as a function of the anatomical locations of breathing sounds recording, * – $p < 0.05$ RP0-20 healthy controls values versus peak disease; ◆– $p < 0.05$ RP0-20 healthy controls values versus pre-discharge; D – pre-discharge; PD – peak disease; RP0-200 – ratio Pn0-200/Pn0-2000;

Table 2
Sensitivity, specificity, and AUC for the 5-fold cross-validations of the different classifiers.

		With RP0-20			Without RP0-20			
		Sensitivity	Specificity	AUC	Sensitivity	Specificity	AUC	P value
HC vs PD	Front	77	76	0.77	75	76	0.72	0.42
	Back	84	91	0.89	74	67	0.77	0.0037
	Front + Back	78	91	0.87	69	81	0.81	0.053
HC vs D	Front	45	76	0.58	54	76	0.59	0.63
	Back	80	71	0.8	61	71	0.69	0.041
	Front + Back	71	95	0.85	51	91	0.71	0.0063
PD vs D	Front	86	57	0.67	52	62	0.53	0.32
	Back	76	71	0.77	57	52	0.54	0.049
	Front + Back	71	81	0.79	62	57	0.55	0.041

AUC – area under curve; D – patients discharged from the hospital; HC – healthy controls; PD – peak disease.

significantly.

Vast amount of research aims to characterize and standardize BS in order to implement automatic, user-independent, diagnosis of pulmonary conditions [7]. This initiative is still in progress as adventitious BS may not be specific to a single lung disorder. In this perspective COVID-19 is not different. Clinicians report COVID-19 patients having normal BS as well as coarse crackles, rhonchi and less frequently wheezing [16]. Our study is preliminary in the sense that we explored the frequencies detected in COVID-19 pneumonia PD and before discharge. The finding that approximately half of the BS power resides in the infrasound range supports clinical findings of rhonchi and coarse crackles. In addition, these low frequency signals may be related to other mechanisms such as vibration of muscles producing the breathing motion or vibrations of the vascular tree [17]. However, this study was not designed to answer these questions, rather to delineate the frequency difference between PD and D. Moreover, this study was not designed to develop optimal classification features. However, using the infrasound range feature RP0-20 as an input for the SVM, we showed that the infrasound range is valuable. In general, it is difficult to compare results of one automatic BS analyses to another [18] as the data are acquired by various means and the classifiers use different features.

4.2. Limitations

This study was limited by the absence of control over the timing of hospitalization of patients; therefore, researchers determined PD according to their clinical evaluation. Critically ill patients were excluded from the study, and therefore conclusions may not be ascribed to such patients. BSR from healthy subjects (not related to the patient group) were used as control. We realize that this group was younger and healthy, and it is possible that the HC group does not accurately represent the COVID-19 patient group prior to contracting SARS-Cov-2. Also, in our COVID-19 group, 2 patients had COPD, whereas the HC group did not. Thus, the difference between the groups may also be due to COPD in addition to COVID-19.

In order to accurately analyze BSR in the frequency domain, one should normalize results to subject's height and velocity of air flow in the trachea [6]. This was impossible to implement with COVID-19 patients, yet practiced previously [14]. It is also acknowledged that the patient group was small and correlating BS power with clinical characteristics, lab and imaging results is lacking. Finally, it is emphasized that our analysis pertains to the specific clinical setting reported here. The usefulness of the VoqX^{TM} device and BS power analysis must be tested in other clinical settings, e.g. outpatient clinics, in order to draw wider conclusions.

5. Conclusions

It was easy to use a Smart stethoscope in a quarantine ward as it combines standard auscultation and means for computerized off-line analyses of BS. Specifically, power analysis of BS is relevant when BS were recorded from auscultation points on the back. The infrasound range improves classification ability. Further studies are required to correlate BS frequencies with clinical manifestations and imaging

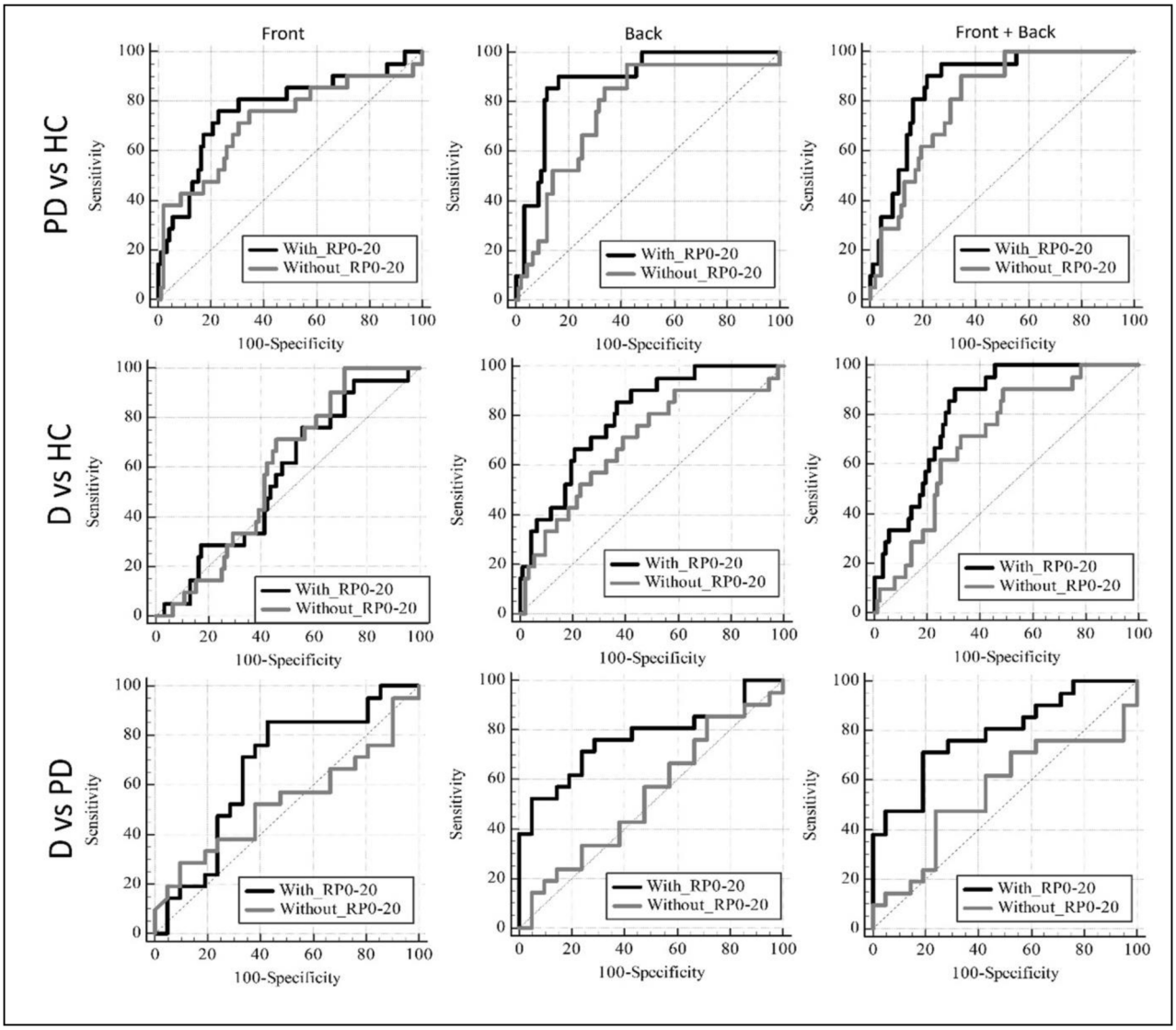

Fig. 5. ROCs for the different classifiers, D – Patients discharged from the hospital; HC – healthy controls; PD – peak disease.

findings.

Funding

The authors have not declared a specific grant for this research from any funding agency in the public, commercial or not-for-profit sectors.

CRediT authorship contribution statement

Nour Kasim: Conceptualization, Investigation, Methodology, Data curation. **Noa Bachner-Hinenzon:** Conceptualization, Formal analysis, Resources, Software, Methodology, Validation. **Shay Brikman:** Investigation, Methodology, Data curation. **Ori Cheshin:** Investigation, Methodology, Data curation. **Doron Adler:** Conceptualization, Resources, Project administration. **Guy Dori:** Formal analysis, Methodology, Conceptualization, Project administration, Investigation, Writing – original draft, Writing – review & editing, Supervision.

Declaration of Competing Interest

The authors declare that they have no known competing financial interests or personal relationships that could have appeared to influence the work reported in this paper.

References

[1] A. Zizza, V. Recchia, A. Aloisi, M. Guido, Clinical features of COVID-19 and SARS epidemics. A literature review, J. Prev Med. Hyg. 62 (2021) E13–E24, https://doi.org/10.15167/2421-4248/jpmh2021.62.1.1680.

[2] N.a. Zhu, D. Zhang, W. Wang, X. Li, B.o. Yang, J. Song, X. Zhao, B. Huang, W. Shi, R. Lu, P. Niu, F. Zhan, X. Ma, D. Wang, W. Xu, G. Wu, G.F. Gao, W. Tan, A Novel Coronavirus from Patients with Pneumonia in China, 2019, N. Engl. J. Med. 382 (8) (2020) 727–733.

[3] D. Wang, B. Hu, C. Hu, F. Zhu, X. Liu, J. Zhang, B. Wang, H. Xiang, Z. Cheng, Y. Xiong, Y. Zhao, Y. Li, X. Wang, Z. Peng, Clinical Characteristics of 138 Hospitalized Patients With 2019 Novel Coronavirus–Infected Pneumonia in Wuhan, China, JAMA. 323 (2020) (2019) 1061–1069, https://doi.org/10.1001/JAMA.2020.1585.

[4] B. Wang, Y. Liu, Y. Wang, W. Yin, T. Liu, D. Liu, D. Li, M. Feng, Y. Zhang, Z. Liang, Z. Fu, S. Fu, W. Li, N. Xiong, G. Wang, F. Luo, Characteristics of Pulmonary Auscultation in Patients with 2019 Novel Coronavirus in China, Respiration. 99 (2020) (2019) 755–763, https://doi.org/10.1159/000509610.

[5] B.H. Tan, Y. Zhang, Y. Gui, S. Wu, Y.C. Li, The possible impairment of respiratory-related neural loops may be associated with the silent pneumonia induced by SARS-CoV-2, J. Med. Virol. 92 (2020) 2269–2271, https://doi.org/10.1002/jmv.26158.

[6] V. Gross, A. Dittmar, T. Penzel, F. Schüttler, P. Von Wichert, The relationship between normal lung sounds, age, and gender, Am. J. Respir. Crit. Care Med. 162 (2000) 905–909, https://doi.org/10.1164/ajrccm.162.3.9905104.

[7] R.X.A. Pramono, S. Bowyer, E. Rodriguez-Villegas, Automatic advetitious respiratory sound analysis: a systematic review, PLoS ONE 12 (2017) e0177926.

[8] S. Reichert, R. Gass, C. Brandt, E. Andres, Analysis of respiratory sounds: state of the art, Clin. Med. Circ. Respirat. Pulm. Med. 16 (2008) 45–58.

[9] E.A. Lapteva, O.N. Kharevich, V.V. Khatsko, N.A. Voronova, M.V. Chamko, I. V. Bezruchko, E.I. Katibnikova, E.I. Loban, M.M. Mouawie, H. Binetskaya, S. Aleshkevich, A. Karankevich, V. Dubinetski, J. Vestbo, A.G. Mathioudakis, Automated lung sound analysis using the LungPass platform: a sensitive and specific tool for identifying lower respiratory tract involvement in COVID-19, Eur Respir J 58 (2021) 2101907, https://doi.org/10.1183/13993003.01907-2021. PMID: 34531278; PMCID: PMC8754101.

[10] A. Glangetas, M.A. Hartley, A. Cantais, D.S. Courvoisier, D. Rivollet, D.M. Shama, A. Perez, H. Spechbach, V. Trombert, S. Bourquin, M. Jaggi, C. Barazzone-Argiroffo, A. Gervaix, J.N. Siebert, Deep learning diagnostic and risk-stratification pattern detection for COVID-19 in digital lung auscultations: clinical protocol for a case-control and prospective cohort study, BMC Pulm. Med. 21 (2021) 103, https://doi.org/10.1186/s12890-021-01467-w. PMID: 33761909; PMCID: PMC7988633.

[11] E.R. DeLong, D.M. DeLong, D.L. Clarke-Pearson, Comparing the areas under two or more correlated receiver operating characteristic curves: a nonparametric approach, Biometrics 44 (1988) 837–845.

[12] Y. Kim, Y.K. Hyon, S.S. Jung, S. Lee, G. Yoo, C. Chung, T. Ha, Respiratory sound classification for crackles, wheezes, and rhonchi in the clinical field using deep learning, Sci. Rep. 11 (2021) 17186, https://doi.org/10.1038/s41598-021-96724-7.

[13] C. Yang, W. Zhang, Z. Pang, J. Zhang, D. Zou, X. Zhang, S. Guo, J. Wan, K. Wang, W. Pang, A low-cost, ear-contactless electronic stethoscope powered by raspberry pi for auscultation of patients with covid-19: Prototype development and feasibility study, JMIR Med. Inform. 9 (2021) e22753.

[14] N. Gavriely, M. Nissan, A.H.E. Rubin, D.W. Cugell, Spectral characteristics of chest wall breath sounds in normal subjects, Thorax. 50 (1995) 1292–1300, https://doi.org/10.1136/thx.50.12.1292.

[15] J.-Z. Tsai, M.-L. Chang, J.-Y. Yang, D. Kuo, C.-H. Lin, C.-D. Kuo, Left-right asymmetry in spectral characteristics of lung sounds detected using a dual-channel auscultation system in healthy young adults, Sensors (Switzerland). 17 (6) (2017) 1323.

[16] P. Zhang, B. Wang, Y. Liu, M. Fan, Y. Ji, H. Xu, M. Xu, S. Chen, Q. Li, Z. Zhang, Lung auscultation of hospitalized patients with SARS-CoV-2 pneumonia via a wireless stethoscope, Int. J. Med. Sci. 18 (2021) 1415–1422, https://doi.org/10.2196/22753.

[17] K. Lee, X. Ni, J.Y. Lee, H. Arafa, D.J. Pe, S. Xu, R. Avila, M. Irie, J.H. Lee, R. L. Easterlin, D.H. Kim, H.U. Chung, O.O. Olabisi, S. Getaneh, E. Chung, M. Hill, J. Bell, H. Jang, C. Liu, J.B. Park, J. Kim, S.B. Kim, S. Mehta, M. Pharr, A. Tzavelis, J.T. Reeder, I. Huang, Y. Deng, Z. Xie, C.R. Davies, Y. Huang, J.A. Rogers, Mechano-acoustic sensing of physiological processes and body motions via a soft wireless device placed at the suprasternal notch, Nat. Biomed. Eng. 4 (2) (2020) 148–158.

[18] M. Alkhodari, A.H. Khandoker, R. Damaševičius, Detection of COVID-19 in smartphone-based breathing recordings: A pre-screening deep learning tool, PLoS ONE 17 (1) (2022) e0262448.